

Article - Human and Animal Health

Physicochemical Characterization, Quantitative Drug Analysis, and Stability Testing of Hydroxytyrosol-loaded Poly(ϵ -caprolactone) Nanocapsules

Juliana Parente Menezes Ribeiro¹
https://orcid.org/0000-0002-9405-0644

Jessica Mendes Nadal²
https://orcid.org/0000-0002-2419-2110

Diego José Schebelski^{2*}
https://orcid.org/0000-0001-8647-6760

Andressa Novatski¹
https://orcid.org/0000-0002-8327-6285

Amanda Martinez Lyra²
https://orcid.org/0000-0002-5849-669X

Jane Manfron^{1,2}
https://orcid.org/0000-0003-1873-2253

Guilherme dos Anjos Camargo²
https://orcid.org/0000-0002-3440-2791

Paulo Vitor Farago^{1,2}
https://orcid.org/0000-0002-9934-4027

¹ Universidade Estadual de Ponta Grossa, Programa de Pós-graduação em Ciências da Saúde, Ponta Grossa, Paraná, Brasil; ² Universidade Estadual de Ponta Grossa, Programa de Pós-graduação em Ciências Farmacêuticas, Ponta Grossa, Paraná, Brasil

Editor-in-Chief: Yasmine Mendes Pupo
Associate Editor: Najeh Maissar Khalil

Received: 24-Jan-2023; Accepted: 31-Jan-2023

*Correspondence: diego.ski@hotmail.com; Tel.: + 55 (42) 30284040/991614400 (D.J.S.).

HIGHLIGHTS

- Hydroxytyrosol (HT)-loaded PCL nanocapsules were appropriately obtained and characterized.
- A simple and fast UHPLC method for HT determination in PLC nanocapsules was developed and validated.
- High HT encapsulation efficiency was achieved into the PCL nanocapsule formulations.
- HT-loaded PCL nanocapsules showed physicochemical stability from 30 to 90 days.

Abstract: Hydroxytyrosol (HT) is a natural phenolic compound found in leaves of olive trees. It is a photosensitive solid phytochemical constituent and an irritant substance to skin and mucosa as pure drug. HT is a lipophilic chemical constituent and shows low solubility in water, bitter taste, and instability to oxidizing atmosphere. Considering the limitations for its suitable therapeutic use, the aim of the present study was to obtain, to characterize, to quantify, and to evaluate the stability of HT-loaded poly(ϵ -caprolactone) nanocapsules for its further use in pharmaceutical and nutraceutical products. Nanocapsules were prepared by method of interfacial deposition of the preformed polymer. The formulations were characterized by morphological and spectroscopic methods. The UHPLC-PDA analytical method was developed and validated for quantifying the HT encapsulation. Physicochemical stability assay was performed for 120 days. Nanocapsules were successfully obtained by the proposed method. The morphological evaluation demonstrated the drug absence in the nanocapsule surface. Fourier-transform infrared spectroscopy

demonstrated the drug nanoencapsulation. The analytical method was validated and confirmed a high HT encapsulation efficiency over 95%. Considering the physicochemical stability testing, the polydispersity index changed after 30 days for NC-2 (HT at 2 mg/mL) and after 90 days for NC-5 (HT at 5 mg/mL). Zeta potential changed after 60 days for both formulations (NC-2 and NC-5). pH values were modified after 60 days for NC-5 and after 90 days for NC-2. HT-loaded PCL nanocapsules demonstrate adequate physicochemical features and high drug encapsulation. The different formulations revealed stability changes from 30 to 90 days. Additional in vitro and in vivo evaluations may be performed in order to use these nanoformulations for treating several diseases based on oxidative-inflammatory environments.

Keywords: antioxidant; nanotechnology; *Olea europaea*; oleuropein; polyphenol.

INTRODUCTION

Hydroxytyrosol (HT) or (3,4-dihydroxyphenylethanol) ($C_8H_{10}O_3$) is a photosensitive solid compound that is irritant to skin and mucosa [1-4]. It has a molecular weight of 154.16 g/mol, melting point at 355.40°C and low solubility in water: 50 mg/mL (25°C) [1,4]. It belongs to the organic class of compounds known as tyrosols, a member of the catechol group and it is a primary alcohol [1,4]. It is isolated from *Olea europaea* L. [5,6] and is found in leaves of the olive tree [7] after the hydrolysis of oleuropein, which is enzymatically and/or chemically degraded (Figure 1) [3,8]. It has pharmacological properties, such as antioxidant [7,9,10], antimicrobial [8,10], antiviral [11], anti-inflammatory [7,8,10,11], antithrombotic [8,10] and anticancer [8,10,11] properties. HT can be found in a number of foods, such as olives and their oil and grape derivatives [8,12,13].

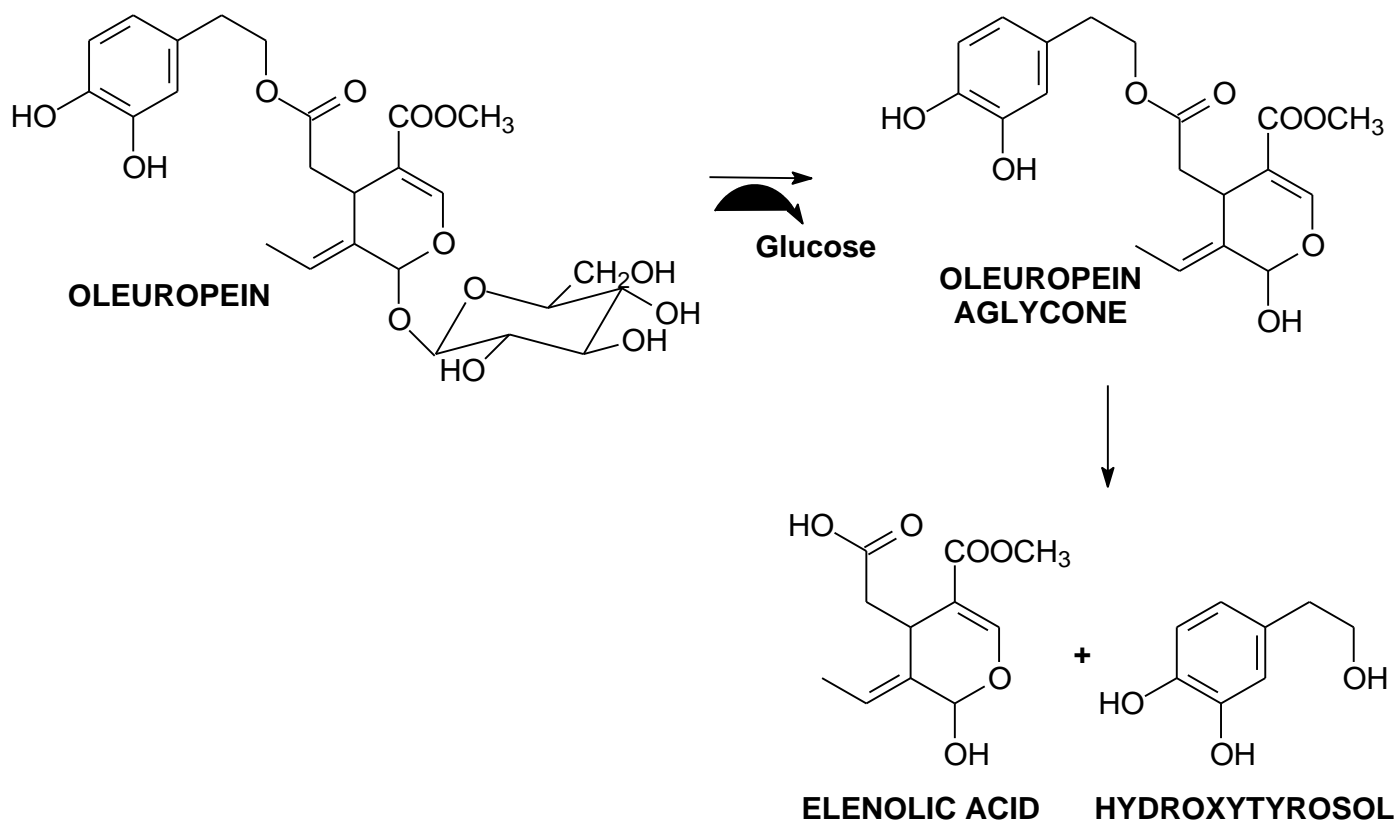


Figure 1. Chemical obtention of HT from oleuropein

Bioactive properties of HT are achieved through several biochemical mechanisms involving the regulation of xenobiotic pathways, interleukins, prostaglandins, transcription factors, and antioxidant enzymes (SOD, catalase, glutathione peroxidase) [4,14,15].

Due to its low solubility in water, photosensitivity and irritating features to the skin and the mucous membranes, nanoencapsulation is an interesting technological alternative to overcome these inconveniences. One of the possible strategies is to obtain poly(ϵ -caprolactone) (PCL) nanocapsules that present particular characteristics, such as biodegradability and non-toxic profile, which make them ideal carriers for HT [16-18].

In addition, there are few studies about nanocapsules containing HT as a pure drug. In general, HT was incorporated into polymeric systems as olive leaf and olive oil extracts, and the HT quantification was not rigorously considered since other drugs or substances were also presented [5,19-21].

Therefore, this study aimed to obtain and to characterize HT-loaded PCL nanocapsules (NCs). In addition, a reversed-phase UHPLC-photodiode array (RP-UHPLC-PDA) method to quantify HT into NCs was also developed and validated. The physicochemical stability of the colloidal suspensions of NCs was also performed.

MATERIAL AND METHODS

Materials

Hydroxytyrosol 98.99% pure (Abacipharm Corporation, Columbia, MD, USA), poly(ϵ -caprolactone) (PCL) ($M_w = 14,000$ g/mol, Sigma-Aldrich, St. Louis, MO, USA), sorbitan monooleate (Span 80, Oxiteno, Mauá, Brazil), polysorbate 80 (Tween 80, Delaware, Porto Alegre, Brazil), medium chain triglycerides (MCT, 99% pure, Focus Química, São Paulo, Brazil), lactose monohydrate (LAC, Biotec Produtos Químicos, São José dos Pinhais, Brazil), acetone (99.9% pure, Vetec Química, Rio de Janeiro, Brazil), Methanol HPLC grade (Research Hexis, Phillipsburg, NJ, USA), acetone P.A. (Synth, Diadema, Brazil), Acetonitrile HPLC grade (J.T. Baker, Phillipsburg, NJ, USA) were used as received. Water was purified in a Milli-Q Plus water purification system (Millipore, Bedford, MA, USA).

Preparation of HT-loaded PCL nanocapsules

HT-loaded poly(ϵ -caprolactone) nanocapsule suspensions were prepared by interfacial deposition of preformed polymer method [22-25]. Briefly, PCL (0.100 g) was solvated in acetone (27 mL) in the presence of Span 80 (0.0770 g), HT (0.020 or 0.050 g), and MCT (0.300 g) until solubilization under mechanical stirring at 3.500 rev/min and 40°C (Fisaton equipment, 713 model, São Paulo, Brazil). The organic phase was then dripped onto the aqueous phase (53 mL) containing Tween 80 (0.0770 g). The mixture was kept under mechanical stirring at 3.500 rev/min at 40 °C for 10 min. The organic solvent was evaporated under reduced pressure in a rotary evaporator (Tecnal, TE-211 model, Piracicaba, Brazil) to the final volume of 10 mL for obtaining the loaded formulation at 2 mg/mL (NC-2) or 5 mg/mL (NC-5) of HT. The experiment was carried out from six different batches. For comparative purposes, a suspension of nanoparticles was prepared with no HT (NC-0) [26].

Characterization of HT-loaded PCL nanocapsules

pH Determination

The pH value was obtained in a digital potentiometer (Hanna, HI 2221, São Paulo, Brazil) previously calibrated with pH 4.0 and 7.0 buffer solutions, directly in each colloidal suspensions after their preparation. Results were represented as the mean from the six different batches.

Determination of Mean Diameter, Polydispersity Index (PDI), and Zeta Potential of NCs

Mean diameter, PDI, and zeta potential were measured ($n = 6$) by photon correlation spectroscopy (PCS) according to dynamic light scattering (DLS) after diluting an aliquot of the NCs in ultrapurified water (1:500) (Zetasizer Nanoseries, Malvern Instruments, Malvern, UK). A one-way analysis of variance (ANOVA) followed by Tukey's post-hoc test was performed to verify the statistical difference between the mean values.

Field Emission Scanning Electron Microscopy (FESEM)

Morphological and surface evaluation of the raw materials and NCs was performed by Field Emission Scanning Electron Microscopy (FESEM) (Tescan, Mira 3 model, Brno, Czech Republic) at an acceleration voltage of 10 to 15 kV [27, 28]. Samples were previously subjected to metallization with gold in an IC-50 Ion metallizer Coater (Shimadzu, Kyoto, Japan) [29].

Fourier-Transform Infrared Spectroscopy (FTIR)

The formulations were analyzed by FTIR using potassium bromide (KBr) pellets, using 4 mg of each sample and 196 mg of spectroscopic grade KBr (2%, m/m) in the IR Prestige-21 equipment (Shimadzu,

Kyoto, Japan) at the range of 4000–500 cm⁻¹ with a resolution of 2 cm⁻¹ and 64 scan/min [30]. The spectra obtained were evaluated against the spectra of the pure HT, PCL, physical mixture (PM), and NC-0.

Chromatographic conditions

Experiments were performed in a Shimadzu Nexera System UHPLC, equipped with a quaternary pump (LC-30AD), degasser (DGU-20A), automatic sampler (SIL-30 AC), thermostatic column compartment (CTO-20AC), and a photodiode array detector (SPD-M20A). The analytical column used was a Shimadzu Shim-pack XR-ODS III (C18; 200 mm internal diameter x 2.0 mm x particle size of 2.2 μm). The isocratic mobile phase consisted of methanol: acetonitrile: ultrapure water containing 0.01% formic acid (40:40:20 v/v) with a flow rate of 0.45 mL/min. Temperature of 35°C, injection volume of 10 μL, and wavelength detection at 280 nm were used. The total analytical run time was 2.0 min. The acquisition and processing of the data were obtained with the LabSolutions Software (Shimadzu, Japan).

Preparations of standard solutions and samples

A stock standard solution of 500 μg/mL of HT was daily prepared. This solution was further diluted in the mobile phase to prepare seven different standard solutions ranging from 10 to 100 μg/mL. Final solutions were filtered through a polytetrafluorethylene membrane filter (Chromafil Xtra PTFE-20/13 membrane, 0.20 μm pore size, Macherey-Nagel, Düren, Germany) before injection into the UHPLC system.

Method validation

The UHPLC method was validated according to the guidelines set on The International Conference on Harmonization of Technical Requirements for Registration of Pharmaceuticals for Human Use [23,31,32]. Parameters evaluated were selectivity, linearity and range, limit of detection (LOD), limit of quantification (LOQ), precision, accuracy, and robustness.

Selectivity was determined by analyzing the chromatograms of HT-loaded NCs compared to those obtained from non-loaded formulations. The linearity was investigated by the linear regression using the least squares method from three authentic analytical curves obtained at 10, 25, 40, 55, 70, 85, and 100 μg/mL. The slope and other parameters of the analytical curves were calculated by the linear regression and ANOVA. The residues analysis was carried out using the Statistica 8.0 (StatSoft, Tulsa, OK, USA). The limit of detection (LOD) (Equation 1) and the limit of quantification (LOQ) (Equation 2) were determined using the following equations as recommended by ICH [31]. Where SD is the standard deviation from the response and S is the slope of the mean calibration curve.

$$LOD = \frac{3.3 \times SD}{S} \quad (1)$$

$$LOQ = \frac{10 \times SD}{S} \quad (2)$$

Precision was assessed at two different levels: repeatability (intraday precision) and intermediate precision (interday precision). These parameters were investigated at 55 μg/mL in sextuplicate and at 20, 50, and 80 μg/mL in triplicate. The results were expressed in terms of relative standard deviation (RSD). Accuracy was assessed by recovery analysis in which a known amount of HT (5.0 μg) was added in triplicate to the solutions of 30.0, 60.0, and 80.0 μg/mL. The accuracy of the method was calculated by the percentage ratio between the experimental concentration and the theoretical concentration, and the results expressed as a percentage of recovery. Robustness was evaluated in the samples at 55 μg/mL by intentionally varying the flow rate to 0.445 and 0.455 mL/min, the concentration of the acidified ultrapure water:methanol+acetonitrile mobile phase to 19:81 (v/v) and 21:79 (v/v) and the temperature of analytical column to 33 and 37°C.

Preparations of sample solutions

The final dosage form, a nanopowder, was resuspended in 10 mL of purified water. The nanosuspension (500 μL) was submitted to ultrafiltration in an Amicon device (Mw cutoff = 10,000 g/mol, Merck Millipore, Burlington, MA, USA) by centrifugation at 2,200 rcf for 30 min. The amount of free HT in ultrafiltrate was chromatographically quantified as proposed. All procedures were performed in triplicate.

Method applicability: Evaluation of Encapsulation Efficiency

The amount of HT was calculated and reported as encapsulation efficiency (EE) following Equation 3. EE% was determined from the sample solution. Non-entrapped HT was quantified in the ultrafiltrate by the proposed chromatographic method [23,32].

$$EE(\%) = \frac{\text{theoretical drug content} - \text{free drug content}}{\text{theoretical drug content}} \times 100 \quad (3)$$

Statistical analysis

All data were expressed as mean \pm standard deviation (SD). The linearity data were evaluated by simple linear regression. Relative standard deviation (RSD) was shown as required. Data were compared by ANOVA with Tukey's post-hoc test at a significance level of 5% ($\alpha = 0.05$) [33]. GraphPad Prism software version 5.03 (San Diego, CA, USA) was used for statistical analysis.

Physicochemical stability testing

Suspensions of NCs (NC-2 and NC-5) were stored at cooling ($5 \pm 2^\circ\text{C}$) and protected from light into amber glass bottles. The formulations were monthly monitored during 120 days of storage by checking pH, particle size, PDI, and zeta potential [16]. Particle size and zeta potential were determined by the Zetasizer Nanoseries equipment (Malvern Instruments, NANO ZS 90 model, Malvern, United Kingdom) after a 1:500 dilution using ultrapure water. All samples were assayed in triplicate. All data resulting from stability testing were analyzed using the GraphPad Prism software, 6.01 version for Windows. All data were expressed as mean \pm standard deviation (SD). Student's t-test with Tukey's post-hoc test was used for statistical comparisons at a significance level of 5% ($\alpha = 0.05$).

RESULTS

Preparation of HT-loaded PCL nanocapsules

HT-loaded PCL NCs (NC-2 and NC-5) and the negative control (NC-0) were successfully obtained by the interfacial deposition method of the preformed polymer. All formulations presented a milky aspect and after preparation.

Characterization of HT-loaded PCL nanocapsules

pH Determination

Table 1 shows the pH values for NCs after their preparation.

Table 1. pH values achieved after obtaining the NC formulations

Formulation	Mean	SD*
NC-0	6.10	± 0.35
NC-2	6.12	± 0.10
NC-5	5.99	± 0.02

*SD = standard deviation (n = 6)

Determination of Mean Diameter, Polydispersity Index (PDI), and Zeta Potential of NCs

Mean diameter, PDI, and zeta potential results for the loaded and non-loaded PCL NCs are presented in Table 2.

Table 2. Values obtained for mean diameter, PDI and zeta potential for NCs

Formulation	Mean diameter (nm)		PDI		Zeta Potential (mV)	
	Mean*	SD**	Mean*	SD**	Mean*	SD**
NC-0	271.17	± 1.07	0.20	± 0.01	-47.40	± 8.20
NC-2	279.80	± 3.46	0.22	± 0.00	-44.85	± 2.47
NC-5	267.50	± 3.77	0.19	± 0.03	-40.55	± 3.61

*1-way ANOVA statistical test. **SD = standard deviation (n = 6).

Field Emission Scanning Electron Microscopy (FESEM)

FESEM images are shown in Figure 2. HT (Figure 2a) presented a crystalline and irregular surface. PCL (Figure 2b) showed particles with a slightly irregular surface. PM revealed the presence of both raw materials (Figure 2c). NCs exhibited a slightly irregular spherical shape with a smooth and uniform surface (NC-2, Figure 2d).

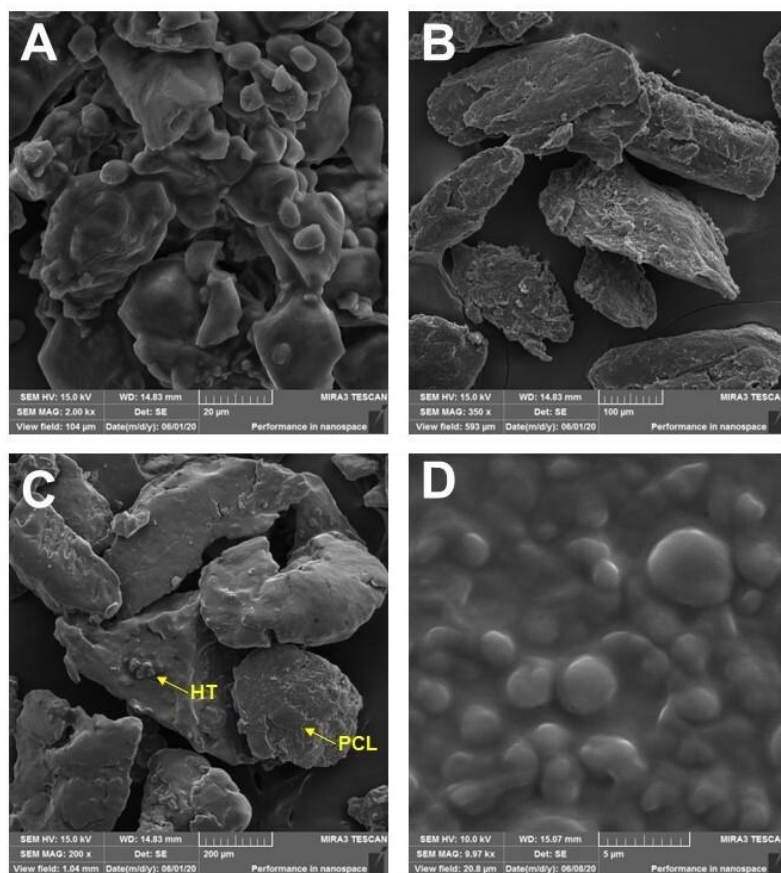


Figure 2. FESEM images of (A) HT pure at 2,000x magnification; (B) PCL pure at 350x magnification; (C) PM (HT:PCL) at 200x magnification, and (D) NC-2 at 9,970x magnification.

Fourier-Transform Infrared Spectroscopy (FTIR)

Figure 3a shows the FTIR spectrum of pure HT. A broad signal assigned to the OH stretching band was observed at $3,357\text{ cm}^{-1}$. sp^3 Hybridized carbon stretching vibrations at $2,953$ and $2,880\text{ cm}^{-1}$, 1,2,4-trisubstituted overtones in aromatic ring between $1,727$ and $1,689\text{ cm}^{-1}$, and aromatic vibrations at $1,610$ and $1,530\text{ cm}^{-1}$ were also verified as previously reported in the literature [21,34]. PCL spectrum (Figure 3b) demonstrated the sp^3 hybridized carbon stretching vibration bands at $2,948$; $2,899$; and $2,865\text{ cm}^{-1}$, the ester $\text{C}=\text{O}$ stretching vibrations at $1,729\text{ cm}^{-1}$, the sp^3 hybridized carbon angular vibration at $1,473\text{ cm}^{-1}$, the $\text{C}-\text{O}$ symmetrical stretching vibrations at $1,297$ and $1,241\text{ cm}^{-1}$, the $\text{C}-\text{O}$ asymmetrical stretching vibration at $1,175\text{ cm}^{-1}$, and the sp^3 hybridized carbon angular vibration at 731 cm^{-1} as observed in others studies [21,35]. Figure 3c depicts the FTIR spectra of PM, non-loaded (NC-0) and loaded (NC-2 and NC-5) NCs. The absorption bands assigned to PM correspond to the superposition of the both FTIR spectra of the raw materials (HT and PCL), mainly because the PCL carbonyl band appears in $1,722\text{ cm}^{-1}$. NCs spectra revealed the carbonyl stretching vibration band ($\text{C}=\text{O}$) [36] at $1,633\text{ cm}^{-1}$ as the main apparent assignment.

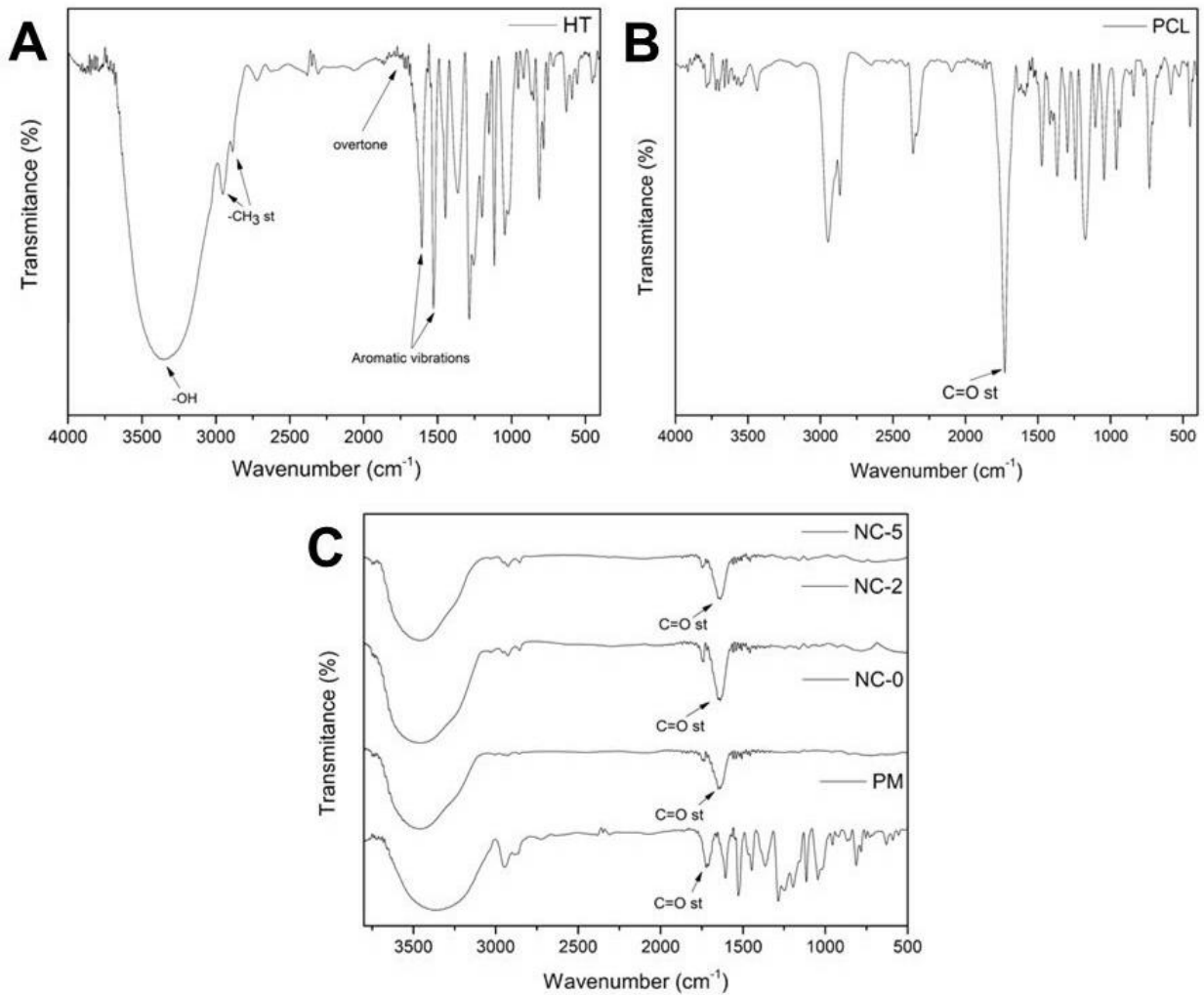


Figure 3. FTIR spectra of HT (a), PCL (b), physical mixture, non-loaded, and HT-loaded nanocapsules (c).

Method validation

Method was validated using methanol:acetonitrile:ultrapure water containing 0.01% formic acid (40:40:20 v/v) as mobile phase and a flow rate of 0.45 mL/min. The retention time and the total analysis time were 2.0 and 2.5 min, respectively.

Specificity was demonstrated by comparing the chromatograms obtained for non-loaded NCs and pure HT. Results showed that there was no interference in the retention time of HT from the other formulation components. In that sense, it is possible to confirm the specificity of the proposed method (Figure 4).

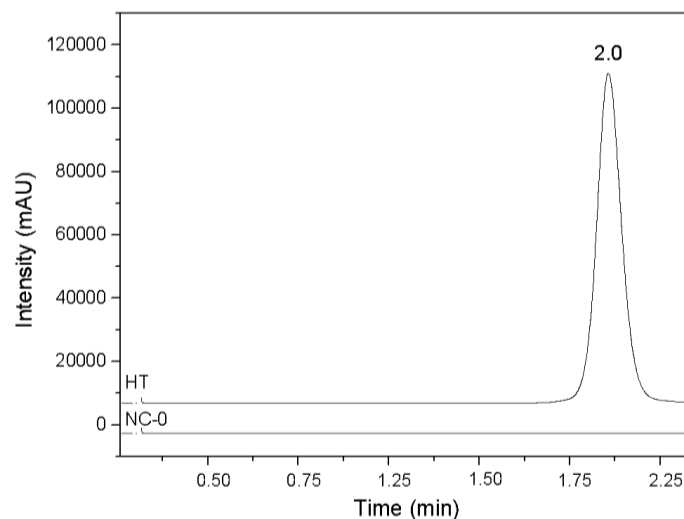


Figure 4. Representative chromatogram of pure HT and NC-0 formulation.

Linearity was performed in triplicate in the concentration range from 10 to 100 µg/mL. The linear equation achieved was $y = 15168.1x - 32890.6$, where y is the peak area and x is the standard solution concentration in µg/mL. A correlation coefficient of $r = 0.9996$ was recorded, which suggested that the method was linear since an r value close to 1.0 could indicate the calibration curve suitability [23,27] (Figure 5).

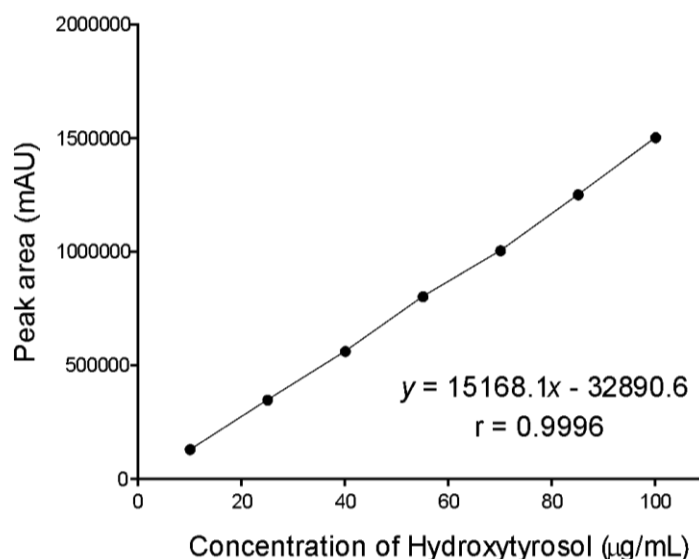


Figure 5. Graphical representation of the mean analytical curve obtained to quantify HT by RP-UHPLC-PDA method at a concentration range from 10 to 100 µg/mL.

The RSD of slope was 1.76%, a value lower than that recommended by ICH (5%) [31]. The negative b value (-32890.33) was in the 95% confidence interval of the analytical calibration curve by the ANOVA test. These results are summarized in Table 3.

Table 3. Linearity parameters of the RP-UHPLC-PDA method for quantifying HT from NCs

Linearity	
Linear Range (µg/mL)	10.0 – 100.0 µg/mL
Detection limit (µg/mL)	1.09 µg/mL
Quantification limit (µg/mL)	3.31 µg/mL
Regression data	
N	3
Slope	15168
Standard deviation of slope	267
Relative standard deviation of slope (%)	1.76
Intercept (b)	-32890.33
Correlation coefficient (r)	0.9996

In order to confirm the linearity, the ANOVA test was performed to investigate if the obtained variation is due to the regression or to the error (residuals). The F value obtained for the lack of adjustment was less than the critical F value for a 95% confidence interval ($\alpha = 0.05$) as depicted in Table 4.

Table 4. ANOVA results for linearity of the RP-UHPLC-PDA method for quantifying HT from NCs

HT	SS	DF	MS	F	F_{crit}
Model	4.348351E+12	1	4.348351E+12	8274.273	2.990
Residual	9.985007E+09	19	5.255267E+08	Linear	
Lack of fit	3.742601E+09	5	748520108	1.678725	2.307
Pure error	6.242406E+09	14	445886164	No lack of fit	

SS: sums of squares; DF: degrees of freedom; MS: mean squares; F : F value of the test; F_{crit} : critical F value.

The developed method showed a LOD and a LOQ of 1.09 and 3.31 µg/mL, respectively.

Precision data were expressed as relative standard deviation (RSD) obtained for repeatability and intermediate precision are described in Table 5.

Table 5. Results of precision assays of the RP-UHPLC-PDA method for quantifying HT from NCs.

Precision	Theoretical concentration ($\mu\text{g/mL}$)	Experimental concentration ($\mu\text{g/mL}$, mean \pm SD*)	RSD** (%)
Repeatability			
n = 6	55	55.07 \pm 0.34	0.61
n = 3	20	20.55 \pm 0.25	1.24
n = 3	50	49.05 \pm 0.16	0.32
n = 3	80	79.90 \pm 1.13	1.42
Intermediate Precision			
Intraday			
n = 6	55	54.87 \pm 0.40	0.74
n = 3	20	20.41 \pm 0.27	1.34
n = 3	50	48.80 \pm 0.33	0.67
n = 3	80	79.56 \pm 1.03	1.29
Interday			
n = 6	55	55.34 \pm 0.49	0.89
n = 3	20	20.55 \pm 0.23	1.10
n = 3	50	49.08 \pm 0.16	0.32
n = 3	80	79.90 \pm 0.99	1.24
Different analyst			
n = 6	55	55.44 \pm 0.56	1.01
n = 3	20	20.46 \pm 0.26	1.29
n = 3	50	49.46 \pm 0.47	0.95
n = 3	80	79.60 \pm 1.02	1.28

*SD = standard deviation; **RSD = relative standard deviation

Accuracy recovery rate of HT was between 91.10 and 102.31% for the different concentration levels evaluated. Table 6 describes the obtained data.

Table 6. Results of accuracy assays of the RP-UHPLC-PDA method for quantifying HT from NCs

Level of concentration	Final HT concentration ($\mu\text{g/mL}$)	SD (% \pm SD*)	RSD** (%)
Low	35	91.10 \pm 3.17	3.48
Medium	65	102.31 \pm 4.80	4.69
High	85	97.14 \pm 2.10	2.16

*SD = standard deviation; **RSD = relative standard deviation.

Robustness was based on the RSD values obtained by changing analytical parameters, such as the flow rate, mobile phase composition and column temperature [31]. The RSD results depicted in Table 7 show that there was no significant difference in the peak area and the HT retention time after the proposed changes.

Table 7. Results of robustness assays of the RP-UHPLC-PDA method for quantifying HT from NCs

Initial parameter	Change	RSD* (%)
Flow rate	0.445 $\mu\text{g/mL}$	0.87
0.45 $\mu\text{g/mL}$	0.455 $\mu\text{g/mL}$	1.09
Mobile phase proportion	19:81 (v/v)	0.67
20:80 (v/v)	21:79 (v/v)	1.11
Temperature	33 $^{\circ}\text{C}$	0.67
35 $^{\circ}\text{C}$	37 $^{\circ}\text{C}$	1.15

*RSD = relative standard deviation.

Method applicability: Determination of HT loading efficiency

The drug content and the HT encapsulation efficiency (EE) in PCL nanocapsules was carried out by the previously validated UHPLC-PDA method and the obtained results are represented in Table 8. High drug entrapments were achieved for loaded NCs, which led to EE values higher than 95%.

Table 8. HT loading and encapsulation efficiency for PCL nanocapsules using the validated UHPLC-PDA method

Formulation	Drug loading ($\mu\text{g/mL}$)	Encapsulation efficiency (%)		
		EE	SD ^{***}	RSD ^{****}
NC-2*	1,904.51 \pm 0.81	95.2	\pm 0.00	0.01
NC-5**	4,904.47 \pm 3.82	98.1	\pm 0.01	0.01

*Theoretical concentration (2000 $\mu\text{g/mL}$).

** Theoretical concentration (5000 $\mu\text{g/mL}$).

***SD: standard deviation.

****RSD = relative standard deviation.

Physicochemical stability

Figure 6 illustrates the changes in pH values for the 30-60-90-120-day stability analysis. Significant difference in pH for the HT-loaded formulations started on day 60. The non-loaded formulation NC-0 showed significant change in pH on day 90.

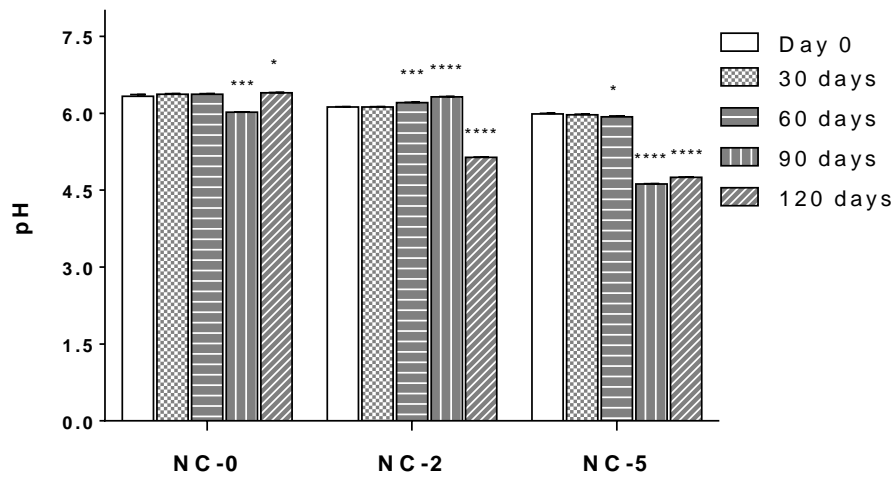


Figure 6. pH values, immediately after preparation and after 30, 60, 90, and 120 days. Negative control (NC-0); HT-loaded PCL NCs containing 2.0 mg/mL of HT (NC-2); HT-loaded PCL NCs containing 5.0 mg/mL of HT (NC-5). Student's t-test with Tukey's post-hoc test, with significance of * $p < 0.05$; *** $p < 0.001$; **** $p < 0.0001$.

Figure 7 demonstrates that there was a statistically significant difference in particle size mainly for NC-2 during the physicochemical stability assay. No change in particle size was achieved for formulation NC-5.

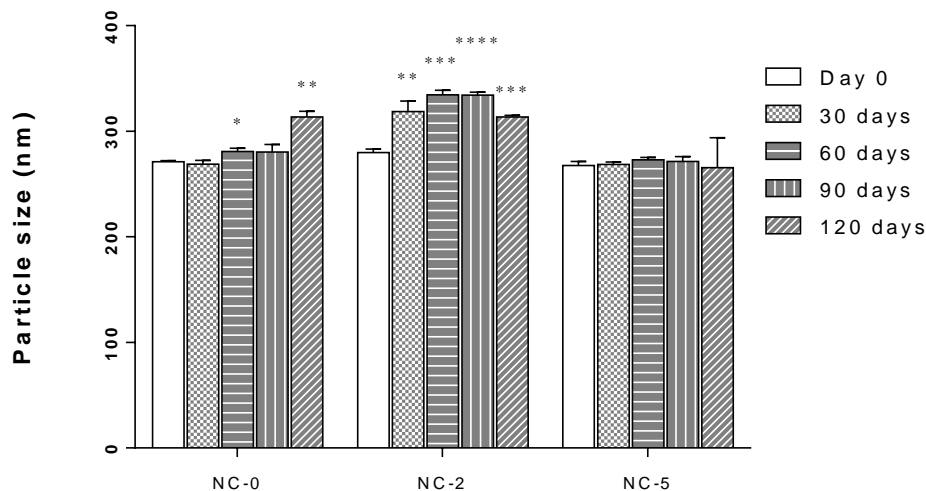


Figure 7. Particle size values, immediately after preparation and after 30, 60, 90, and 120 days. Negative control (NC-0); HT-loaded PCL NCs containing 2.0 mg/mL of HT (NC-2); HT-loaded PCL NCs containing 5.0 mg/mL of HT (NC-5). Student's t-test with Tukey's post-hoc test, with significance of * $p < 0.05$; ** $p < 0.01$; *** $p < 0.001$; **** $p < 0.0001$.

PDI had a significant change for NC-0 after 120 days of preparation and for NC-2 after 30 and 60 days of preparation as illustrated in Figure 8.

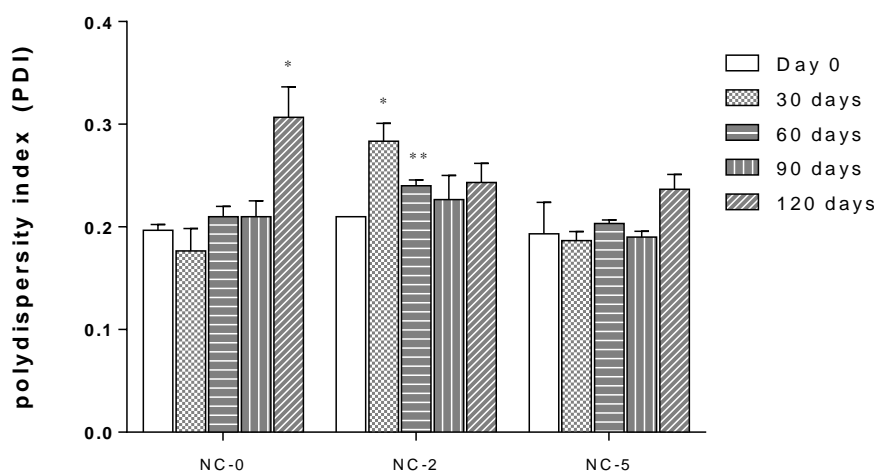


Figure 8. PDI values, immediately after preparation and after 30, 60, 90, and 120 days. Negative control (NC-0); HT-loaded PCL NCs containing 2.0 mg/mL of HT (NC-2); HT-loaded PCL NCs containing 5.0 mg/mL of HT (NC-5). Student's t-test with Tukey's post-hoc test, with significance of * $p < 0.05$; ** $p < 0.01$.

Zeta potential revealed a significant change only for NC-5 after 90 days of preparation (Figure 9). Other samples remained stable for this electrokinetic potential in the colloidal systems.

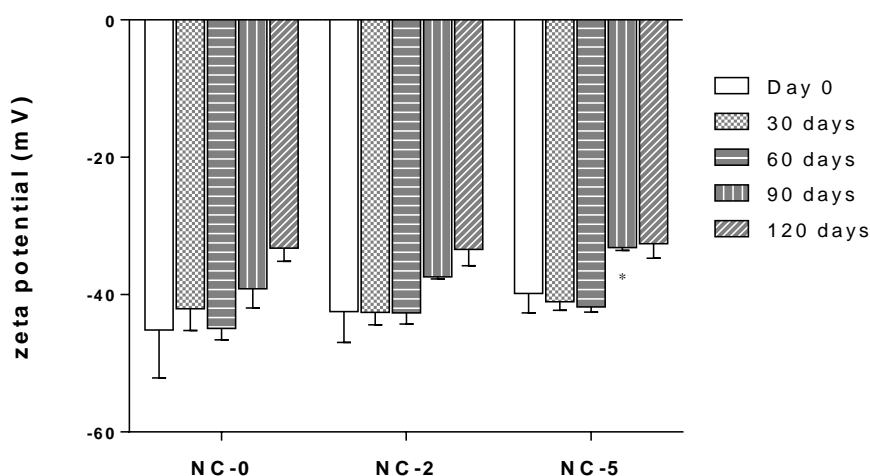


Figure 9. Zeta potential values, immediately after preparation and after 30, 60, 90, and 120 days. Negative control (NC-0); HT-loaded PCL NCs containing 2.0 mg/mL of HT (NC-2); HT-loaded PCL NCs containing 5.0 mg/mL of HT (NC-5). Student's t-test with Tukey's post-hoc test, with significance of * $p < 0.05$.

In addition, all formulations maintained the same initial milky aspect throughout the stability study.

DISCUSSION

HT-loaded PCL nanocapsules showed the usual behavior of other NCs obtained by the same method [36]. HT concentrations used (2 and 5 mg/mL) were chosen considering the usual dosage recommended by FDA [37] and ANVISA [38].

The formulations showed an acid pH value, which was attributed to PCL. This polymer is an aliphatic polyester with terminal carboxyl groups that can undergo hydrolysis generating pH acidification [16,39,40].

FESEM images did not show the presence of the drug on the nanoparticle surface, which indicated the drug encapsulation in agreement with the literature [41].

FTIR spectra of loaded-NCs revealed that there was no novel band related to HT. In addition, FTIR spectra indicated that HT may be entirely encapsulated and that PCL is only attending as a drug carrier [36].

The analytical method developed and validated by RP-UHPLC-PDA proved to be suitable for a fast and precise analysis of HT into PCL nanocapsules. These chromatographic conditions also provided a lower tail size and a more symmetrical peak for the HT quantification when compared to other methods that used HPLC

[42,43]. Hence, the linearity was confirmed due to the linear regression and did not present a lack of adjustment according to the ANOVA test. LOD and LOQ results represented that the chromatographic method is suitable enough to detect and quantify HT at the concentration range of 10.0 to 100.0 µg/mL. All the RSD values were below 5%, which confirm an appropriate precision for the evaluated method [31]. These results demonstrated that the method is accurate since it is in agreement with the accuracy target limits of 95–105% [31]. Thereby, the RP-UHPLC-PDA method proved to be robust for analyzing HT even at small changes in chromatographic parameters.

High values of encapsulation efficiencies (EEs), over 95%, were obtained in this study for the HT-loaded PCL nanocapsules. The current results are similar or better than the previously reported. HT-loaded poly(lactic) acid nanoparticles coated with β-cyclodextrin polymer revealed an EE value of 92.6% [44]. Liposomes containing water-soluble HT demonstrated mean EE value of 45.08% [45]. HT in chitosan nanoparticles prepared by ionic crosslinking reached EE values between 33% and 63% [46].

Mean particle size between 267.50 nm (NC-5) and 279.80 nm (NC-2) were achieved for the NC formulations. According to the statistical test performed, there is no significant difference between these formulations. Several previous studies highlighted that polymeric nanocapsules usually show diameters between 100 and 300 nm and this parameter depends on the formulation composition, the preparation method and the nature of the oil used in the NC core [16,17,47].

Regarding the PDI, all formulations showed values lower than 0.3, which indicates a homogeneous distribution of the size of the polymeric nanocapsules. The zeta potential revealed the electrostatic stability of the nanoparticles, since it reflects the surface potential and must be higher than |30 mV|. The negative value was due to the anionic nature of the polymer PCL [47].

Particle size values and surface properties can play an important role in its bioactivity by influencing the *in vitro* drug release since the smaller particle size leads to a larger surface area, which results in the rapid release of the active substance. On the other hand, the negative characteristic of the surface promotes increased permanence in the blood [39,41,48-50].

The physicochemical stability assay on days 30, 60, 90, and 120 indicated significant changes in pH values of NCs. This effect probably occurred due to the hydrolysis of the medium chain triglycerides, tween 80, and PCL, which released carboxylic groups that increased the polymer degradation and led to the medium acidification [16,41]. NCs have changed their mean size over time and this phenomenon was probably due to the fact that they agglomerate over time [44,51]. Despite the change in PDI, the values remained acceptable below 0.3 [52], which is suitable for pharmaceutical use. Zeta potential remained unchanged, indicating that the NCs maintained the electrical stability over time [44,51].

In addition, the NCs showed macroscopic stability with no cremation, sedimentation or flocculation [16,44,47]. Thus, the physical-chemical stability testing demonstrated stability varying from 30 to 90 days depending on the formulation investigated.

CONCLUSION

In the present study, HT-loaded PCL nanocapsules (NC-2 and NC-5) and negative control (NC-0) were successfully obtained by the chosen method. Morphological evaluation proved the absence of the drug on the NC surface. NCs presented a smooth surface and a homogeneous size distribution. An adequate mean size and a suitable charge stability were achieved. FTIR showed that there were no chemical reactions between the drug and the polymer during the nanoencapsulation process, indicating that the polymer can carry the drug.

The analytical method validation was achieved for selectivity, linearity, residue analysis, detection limit, quantification limit, repeatability, intermediate precision, accuracy, and robustness. The developed method proved to be adequate for quantifying HT into PCL NCs. In general, stability was demonstrated after 60 days after NCs preparation (NC-5).

Hence, this polymeric nanosystem can be further used as a suitable alternative to overcome the undesired drug features, such as low water solubility, photosensitivity and irritation to skin and mucous membranes. The proposed nanotechnology involves a feasible carrier for HT, which can be used for the most diverse pharmaceutical, nutraceutical and cosmetic applications.

Funding: The authors are grateful to CNPq (grant numbers 313704/2019-8 and 402043/2022-7) and to Araucaria Foundation for financial support.

Acknowledgments: The authors would like to thank the Multi-user Laboratory Complex at the State University of Ponta Grossa for lab facilities.

Conflicts of Interest: The authors declare no conflict of interest.

REFERENCES

1. PubChem National Library of Medicine [Internet]. 2022 Oct. [cited 2022 Oct 01]. Available from: <https://pubchem.ncbi.nlm.nih.gov/compound/Hydroxytyrosol#section=Information-Sources>
2. Silva TS, Ramírez-Carrasco P, Romero-Hasler P, Soto-Bustamante E, Barrera-Arellano D, Robert P, et al. Soybean oil organogelled emulsions as oral delivery systems of hydroxytyrosol and hydroxytyrosol alkyl esters. *Food Chem.* 2022;379:1-8.
3. Bertelli M, Kiani AK, Paolacci S, Manara E, Kurti D, Dhuli K, et al. Hydroxytyrosol: A natural compound with promising pharmacological activities. *J. Biotechnol.* 2020;309:29-33.
4. Wani TA, Masoodi FA, Gani A, Baba WN, Rahmanian N, Akhter R, et al. Olive oil and its principal bioactive compound: Hydroxytyrosol – A review of the recent literature. *Trends in Food Sci. Technol.* 2018;77:77-90.
5. Luzi F, Pannucci E, Clemente M, Grande E, Urciuoli S, Romani A, et al. Hydroxytyrosol and Oleuropein-Enriched Extracts Obtained from Olive Oil Wastes and By-Products as Active Antioxidant Ingredients for Poly (Vinyl Alcohol)-Based Films. *Molecules.* 2021;26:1-20.
6. Salem MB, Affes H, Ksouda K, Sahnoun Z, Zeghal KM, Hammami S. Pharmacological activities of *Olea europaea* leaves. *J. Food Process. Preserv.* 2014;39:3128-36.
7. Takeda R, Koike T, Taniguchi I, Tanaka K. Double-blind placebo-controlled trial of hydroxytyrosol of *Olea europaea* on painin gonarthrosis Phytomedicine. 2013;20:861-4.
8. Granados-Principal S, Quiles JL, Ramirez-Tortosa CL, Sanchez-Rovira P, Ramirez-Tortosa MC. Hydroxytyrosol: from laboratory investigations to future clinical trials. *Nutr. Rev.* 2010;68(4):191-206.
9. Pastor A, Rodríguez-Marató J, Olesti E, Pujadas M, Pérez-Mañá C, Khymenets O, Fitó M, Covas M-I, Solá R, Motilva M-J, Farré M, de la Torre, R. Analysis of free hydroxytyrosol in human plasma following the administration of olive oil. *J. Chromatogr. A.* 2016;1437:183-90.
10. Takeda Y, Bui VN, Iwasaki K, Kobayashi T, Ogawa H, Imai K. Influence of olive-derived hydroxytyrosol on the toll-like receptor 4-dependent inflammatory response of mouse peritoneal macrophages. *BBRC.* 2014;446:1225-1230.
11. Sun Y, Zhou D, Shahidi F. Antioxidant properties of tyrosol and hydroxytyrosol saturated fatty acid esters. *Food Chem.* 2018;245:1262-8.
12. Majumder D, Debnath M, Sharma KN, Shekhawat SS, Prasad GBKS, Maiti D, et al. Olive Oil Consumption can Prevent Non-communicable Diseases and COVID-19: A Review. *Curr. Pharm. Biotechnol.* 2022;23:261-75.
13. Pintado T, Muñoz-González I, Salvador M, Ruiz-Capillas C, Herrero AM. Phenolic compounds in emulsion gel-based delivery systems applied as animal fat replacers in frankfurters: Physico-chemical, structural and microbiological approach. *Food Chem.* 2021;340:1-9.
14. Markovic AK, Toric J, Barbatic M, Brala CJ. Hydroxytyrosol, Tyrosol and Derivatives and Their Potential Effects on Human Health. *Molecules.* 2019;24:1-39.
15. Xie Y-D, Chen Z-Z, Li N, Lu W-F, Xu Y-H, Lin Y-Y, et al. Hydroxytyrosol nicotinate, a new multifunctional hypolipidemic and hypoglycemic agent. *Biomed. & Pharmacother.* 2018;99:715-724.
16. Camargo G dos A, Costa Filha ARC da, Lyra AM, Novatski A, Nadal JM, de Lara LS, et al. Stability testing of tacrolimus-loaded poly(ϵ -caprolactone) nanoparticles by physicochemical assays and Raman spectroscopy. *Vib. Spectrosc.* 2020;110:1-11.
17. Bhattacharya D, Ghosh B, Mukhopadhyay M. Development of nanotechnology for advancement and application in wound healing: a review. *IET Nanobiotechnol.* 2019;13(8):778-85.
18. Abamor ES, Tosyalı OA, Bagirova M, Allahverdiyev A. *Nigella sativa* oil entrapped polycaprolactone nanoparticles for leishmaniasis treatment. *IET Nanobiotechnol.* 2018;12(8):1018-26.
19. García AV, Serrano NJ, Sanahuja AB, Garrigós MC. Novel Antioxidant Packaging Films Based on Poly(ϵ -Caprolactone) and Almond Skin Extract: Development and Effect on the Oxidative Stability of Fried Almonds. *Antioxidants.* 2020;9:1-18.
20. Detsi A, Kavetsou E, Kostopoulou I, Pitterou I, Pontillo ARN, Tzani A, et al. Nanosystems for the Encapsulation of Natural Products: The Case of Chitosan Biopolymer as a Matrix. *Pharmaceutics.* 2020;12:1-48.
21. Beltrán A, Valente AJM, Jiménez A, Garrigós MC. Characterization of Poly(ϵ -caprolactone)-Based Nanocomposites Containing Hydroxytyrosol for Active Food Packaging. *J. Agric. Food Chem.* 2014;62:2244-52.
22. Fessi H, Puisieux F, Devissaguet JP, Ammoury N, Benita S. Nanocapsule formation by interfacial polymer deposition following solvent displacement. *Int. J. Pharm.* 1989;55(1):1-4.
23. Rudnik LAC, Lyra AM, Barboza FM, Klein T, Kanufre CC, Farago PV, et al. PEG-PCL Nanocapsules Containing Curcumin: Validation of HPLC Method for Analyzing Drug-loading Efficiency, Stability Testing and Cytotoxicity on NIH-3T3 Cell Line. *Braz. Arch. Biol. Technol.* 2020;63:1-12.
24. Pilatti LDS, Rodrigues R, Nascimento N da S, Gomes MLS, Zanin SMW, Farago PV, et al. Effect of Cilostazol-Loaded PCL/PEG Nanocapsules on Abdominal Aortic Tunics and Lipid Profile of Wistar Rats. *Braz. Arch. Biol. Technol.* 2020;63:1-7.
25. Lino RC, de Carvalho SM, Noronha CM, Sganzerla WG, da Rosa CG, Nunes MR, et al. Development and Characterization of Poly- ϵ -caprolactone Nanocapsules Containing β -carotene Using the Nanoprecipitation Method and Optimized by Response Surface Methodology. *Braz. Arch. Biol. Technol.* 2020;63:1-12.

26. Chassot JM, Ribas D, Silveira EF, Grünspan LD, Pires CC, Farago PV, et al. Beclomethasone Dipropionate-Loaded Polymeric Nanocapsules: Development, In Vitro Cytotoxicity, and In Vivo Evaluation of Acute Lung Injury. *J Nanosci Nanotechnol*. 2015;15(1):855-64.
27. Machado CD, Raman V, Rehman JU, Maia BHLNS, Meneghetti EK, de Almeida VP, et al. Schinus molle: anatomy of leaves and stems, chemical composition and insecticidal activities of volatile oil against bed bug (*Cimex lectularius*) *Rev. Bras. Farmacogn*. 2019;29(1):1-10.
28. Oberg C, Pochapski MT, Farago PV, Granada CJ, Pilatti GL, Santos FA. Evaluation of desensitizing agents on dentin permeability and dentinal tubule occlusion: an in vitro study. *Gen Dent*. 2009;57(5):496-501.
29. Budel JM, Duarte MR, Farago PV, Takeda IJM. Anatomical characters of the leaf and stem of *Calea uniflora* Less., Asteraceae. *Rev. Bras. Farmacogn*. 2006;16(1):53-60.
30. Almeida MA, Nadal JM, Grassioli S, Paludo KS, Zawadzki SF, Cruz L, et al. Enhanced gastric tolerability and improved anti-obesity effect of capsaicinoids-loaded PCL microparticles. *Mater Sci Eng C Mater Biol Appl*. 2014;1;40:345-56.
31. ICH (2005) Validation of analytical procedures: text and methodology Q2 (R1). International Conference of Harmonization.
32. Camargo GA, Lyra AM, Barboza FM, Fiorin BC, Beltrame FL, Nadal JM, et al. Validation of Analytical Methods for Tacrolimus Determination in Poly(ϵ -caprolactone) Nanocapsules and Identification of Drug Degradation Products. *J. Nanosci. and Nanotechnol*. 2021;21:1-9.
33. Gutiérrez MF, Bermudez J, Dávila-Sánchez A, Alegría-Acevedo LF, Méndez-Bauer L, Hernández M, et al. Zinc oxide and copper nanoparticles addition in universal adhesive systems improve interface stability on caries-affected dentin. *J Mech Behav Biomed Mater*. 2019;100:103366.
34. Bonechi C, Donati A, Tamasi G, Pardini A, Rostom H, Leone G, et al. Chemical characterization of liposomes containing nutraceutical compounds: Tyrosol, hydroxytyrosol and oleuropein. *Biophys. Chem*. 2019;246:25-34.
35. Pupo YM, Farago PV, Nadal JM, Simão LC, Esmerino LA, Gomes OM, et al. Effect of a novel quaternary ammonium methacrylate polymer (QAMP) on adhesion and antibacterial properties of dental adhesives. *Int J Mol Sci*. 2014;15(5):8998-9015.
36. Camargo G dos A, Ferreira L, Schebelski DJ, Lyra AM, Barboza FM, Carletto B, et al. Characterization and In Vitro and In Vivo Evaluation of Tacrolimus-Loaded Poly(ϵ -Caprolactone) Nanocapsules for the Management of Atopic Dermatitis. *Pharmaceutics*. 2021;13(21):1-19.
37. FDA. Guidance for industry: Considering Whether and FDA-Regulated Product Involves the Application of Nanotechnology. [cited 2020 Set]. Available from: <http://www.fda.gov/RegulatoryInformation/Guidances/ucm257698.htm>.
38. Brazil. Ministério da Saúde. Farmacopéia Brasileira. [cited 2020 Set]. Available from: <https://www.gov.br/anvisa/pt-br/assuntos/farmacopeia/farmacopeia-brasileira>.
39. Dimer FA, Friedrich RB, Beck RCR, Guterres SS. Impactos da nanotecnologia na saúde: Produção de medicamentos. *Quím. Nova*. 2013;36(10):1520-6.
40. Mir M, Ishtiaq S, Rabia S, Khatoon M, Zeb A, Khan GM, et al. Nanotechnology: from In Vivo Imaging System to Controlled Drug Delivery. *Nanoscale Res. Lett*. 2017;12(1).
41. Ajiboye AL, Trivedi V, Mitchell JC. Preparation of polycaprolactone nanoparticles via supercritical carbon dioxide extraction of emulsions. *Drug Deliv. Transl. Res*. 2018;8:1790–6.
42. Alzweiri M, Al-Hiari YM. Analysis and Evaluation of Hydroxytyrosol in Olive Leaf Extract. *JJPS*. 2013;6(3):314-22.
43. Smeriglio A, Giovanazzo C, Trombetta D. Development and Validation of RP-HPLC-DAD Method to Quantify Hydroxytyrosol Content in a Semi-Solid Pharmaceutical Formulation. *Med. Chem*. 2015;5(10):442-6.
44. Scoullou Z, Kavvatha T, Roussaki M, Kavetsou E, Papaspyrides C, Vouyiouka S, Anastasia D. Encapsulation of the natural product hydroxytyrosol in poly(lactic)acid nanoparticles coated with β -cyclodextrin polymer. *Anais da 10ª Conferência Científica Panhelênica de Engenharia Química*. 2015.
45. Yuan JJ, Qin FG, Tu JL, Li B. Preparation, Characterization, and Antioxidant Activity Evaluation of Liposomes Containing Water-Soluble Hydroxytyrosol from Olive. *Molecules*. 2017;22(870).
46. Hussain Z, Katas H, Mohd MCA, Kumolosasi E, Buang F, Sahudin S. Self-assembled polymeric nanoparticles for percutaneous co-delivery of hydrocortisone/hydroxytyrosol: an ex vivo and in vivo study using an NC/Nga mouse model. *Int. J. Pharm*. 2013;444(1-2),109-19.
47. Schaffazick S, Stanisçuaski S, De Lucca L, Raffin A. [Characterization and physical-chemical stability of nanoparticulate polymeric systems for drug administration]. *Quim. Nova*. 2003;26:726–37.
48. Peršin Z, Ravber M, Kleinschek KS, Knez Ž, Škerget M, Kurečić M. Bio-nanofibrous mats as potential delivering systems of natural substances. *Tex. Res. J*. 2017;87(4)444-459.
49. Wang W, Li CQ, Hu XL. Developmental expression of beta-glucosidase in olive leaves. *Biol. Plant*. 2009;53(1):138–40.
50. Watkins R, Wu L, Zhang C, Davis RM, Xu B. Natural product-based nanomedicine: recent advances and issues. *Int. J. Nanomedicine*. 2015;28(10):6055-74.

51. Paulo F, Santos L. Encapsulation of the Antioxidant Tyrosol and Characterization of Loaded Microparticles: an Integrative Approach on the Study of the Polymer-Carriers and Loading Contents. *Food Bioproc. Tech.* 2020;13.
52. Gomes MLS, Nascimento NdaS, Borsato DM, Pretes AP, Nadal JM, Novatski A, et al. Long-lasting anti-platelet activity of cilostazol from poly(ϵ -caprolactone)-poly(ethylene glycol) blend nanocapsules, *Mater. Sci. Eng. C.* 2019;94:694-702.



© 2023 by the authors. Submitted for possible open access publication under the terms and conditions of the Creative Commons Attribution (CC BY NC) license (<https://creativecommons.org/licenses/by-nc/4.0/>).